analytical chemistry

Article

pubs.acs.org/ac

Electrical Detection of Nucleic Acid Amplification Using an On-Chip Quasi-Reference Electrode and a PVC REFET

Eric Salm,[†,‡] Yu Zhong,[‡,§] Bobby Reddy, Jr.,[‡,§] Carlos Duarte-Guevara,[‡,§] Vikhram Swaminathan,[‡,∥] Yi-Shao Liu,[⊥] and Rashid Bashir*[,†,‡,§]

[†]Department of Bioengineering, University of Illinois at Urbana−Champaign, Urbana, Illinois 61801, United States

[‡]Micro and Nanotechnology Laboratory, Urbana, Illinois 61801, United States

[§]Department of Electrical and Computer Engineering, University of Illinois at Urbana−Champaign, Urbana, Illinois 61801, United States

[∥]Department of Mechanical Science and Engineering, University of Illinois at Urbana−Champaign, Urbana, Illinois 61801, United States

[⊥]Taiwan Semiconductor Manufacturing Company, Hsinchu, Taiwan

Supporting Information

ABSTRACT: Electrical detection of nucleic acid amplification through pH changes associated with nucleotide addition enables miniaturization, greater portability of testing apparatus, and reduced costs. However, current ion-sensitive field effect transistor methods for sensing nucleic acid amplification rely on establishing the fluid gate potential with a bulky, difficult to microfabricate reference electrode that limits the potential for massively parallel reaction detection. Here we demonstrate a novel method of utilizing a microfabricated solid-state quasi-reference electrode (QRE) paired with a pH-insensitive reference field effect transistor (REFET) for detection of real-time pH changes. The end result is a 0.18 μm, silicon-on-insulator, foundry-fabricated sensor that utilizes a platinum QRE to establish a pH-sensitive fluid gate potential and a PVC membrane REFET to enable pH detection of loop mediated isothermal amplification (LAMP). This technique is highly amendable to commercial scale-up, reduces the packaging and fabrication requirements for ISFET pH detection, and enables massively parallel droplet interrogation for applications, such as monitoring reaction progression in digital PCR.

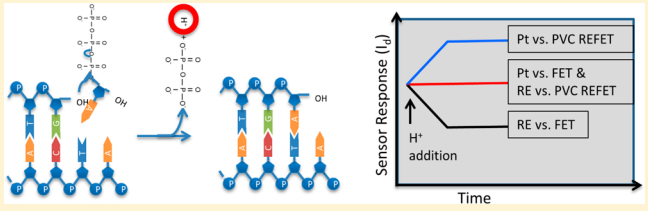

Since the invention of polymerase chain reaction (PCR)-based amplification of nucleic acids by Kary Mullis in 1983,[1] researchers have spent significant efforts to improve the sensitivity and selectivity of PCR assays and have dramatically enhanced its application. PCR is now an integral tool of modern biotechnology processes and biological identification. Because of the growing demands of on-site diagnosis in medicine, realization of point-of-care polymerase chain reaction (PCR) strategies has garnered much attention.[2] Beyond traditional PCR, digital PCR for absolute quantification, increased robustness, and higher sensitivity is highly desirable.[3] Such a strategy would ideally be portable, simple, rapid, have a low cost per test, high accuracy, and reproducibility, require minimal sample volumes and concentrations, and be capable of multiplexed interrogation for many relevant species. Much effort, both academic and commercial, has focused on addressing these challenges, though typically not all at once. In terms of speed, Xxpress[4] offers a qPCR thermal cycler that can achieve 40 cycles of qPCR in less than 10 min, but with a bulky and expensive tabletop system without automation. RainDance[5] and BioRad[6] offer extremely high throughput digital PCR machines utilizing millions of droplets to enable quantification of the initial copy number of the target nucleic acids, but the process takes well over an hour and requires a large table-top system for droplet generation and interrogation. Beyond thermocycling times and droplet technologies, the cost and complexity from fluorescence-based detection limits point-of-care PCR. From a reagent perspective, optical detection requires often proprietary PCR product markers such as SYBR Green or Taqman probes, which can induce inhibitory effects on PCR and increase the per assay cost of each PCR reaction.[7] From an equipment standpoint, optical techniques require bulky components for fluorescence excitation and emission detection. Efforts have focused on miniaturizing these components to bring costs down, but few examples for portable, inexpensive nucleic acid amplification exist.[8,9]

Electrical detection avoids most of these disadvantages by eliminating the need for fluorophores and optical detection equipment entirely. To date, systems utilizing ion sensitive field effect transistors(ISFETs),[10,11] MOS-capacitors,[12] and inter-digitated electrodes[13,14] have demonstrated successful detection of nucleic acid amplification. Of these methods, FET arrays

Received: March 10, 2014
Accepted: June 18, 2014
Published: June 18, 2014

   dx.doi.org/10.1021/ac500897t | *Anal. Chem.* 2014, 86, 6968−6975

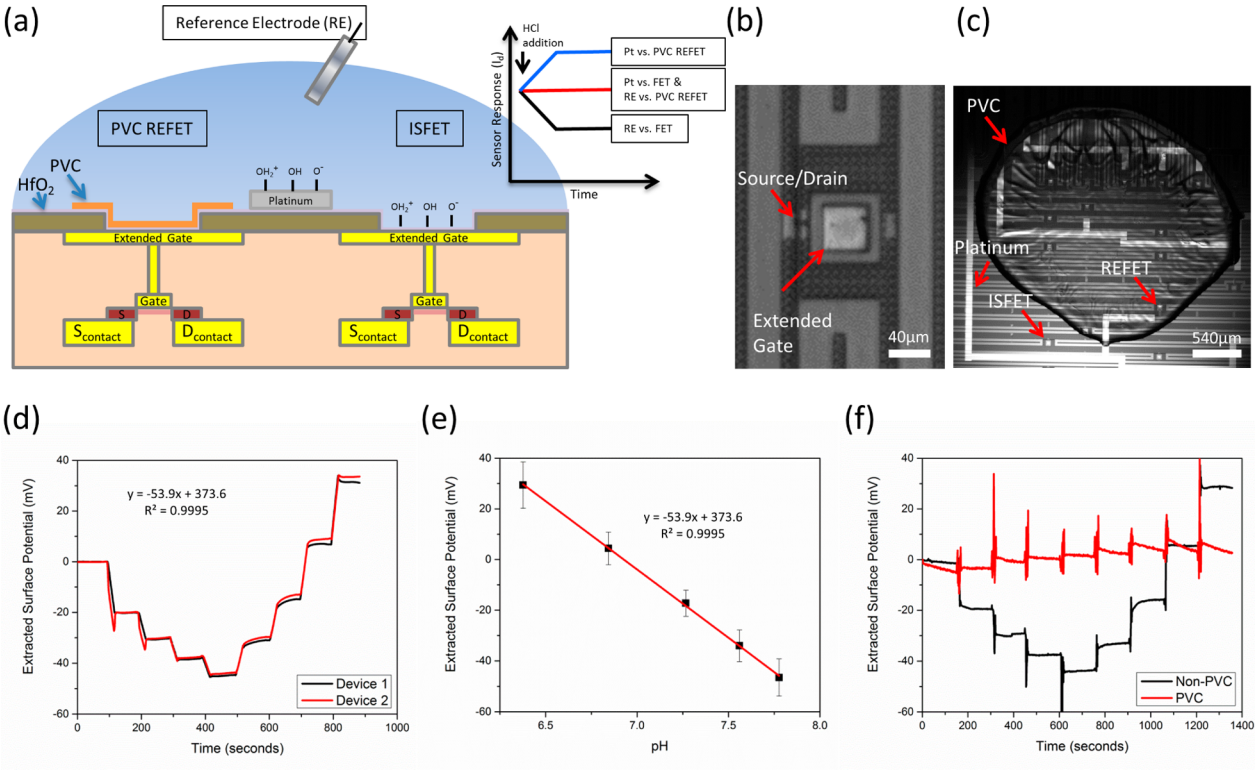

Figure 1. Device schematic and characterization (a) A FET/REFET device schematic is shown. Two fluid gate methods are included: A pH-insensitive reference electrode and a pH-sensitive on-chip platinum electrode. PVC covers the left ISFET, rendering it insensitive to pH changes. The right ISFET is left uncovered and is sensitive to pH. The inset plot shows theoretical device response to a hydrogen addition event. The Pt vs FET and RE vs REFET show no overall response to pH changes. Whereas the Pt vs REFET and RE vs FET show opposite responses. Further details are found in Supporting Information Figure S2. (b) An extended gate ISFET is shown. The sensing region consists of a layer of hafnium oxide on a metal extended gate. (c) One microliter of PVC is spotted on some of the devices to render them pH insensitive, but still functional. (d) A real-time pH response curve of two untreated ISFETs comprising four additions of NaOH followed by four additions of HCl. The response closely matches the Nernstian response for ISFET gate dielectrics with an average pH response of 54 mV/pH and R^2 linearity of 0.995. (e) Quantification of the HCl addition steps for multiple devices is shown (n = 16). (f) Real-time response curve for a RE vs FET (black) and a RE vs PVC REFET (red). The PVC-treated device shows minimal pH response over the duration of the test.

offer benefits of fabrication scalability and row-column addressing for interrogation of millions of individual devices. The ion-sensitive FET (ISFET) sensor system replaces the metal gate of a traditional metal-on-silicon FET with a fluidic interface and a fluid gate electrode. A potential is applied through the fluid via the electrode to operate the device and modulate the FET's source-drain current. Changes in device surface potential through solution pH changes or charged biomolecule addition also cause modulations in the ISFET source-drain current. In traditional operation, a pH-insensitive reference electrode holds the fluid gate constant while the source-drain current is monitored to provide real-time monitoring of solution pH changes. In this paper's design, the changes in surface potential at the ISFET are blocked via a passivating membrane (polyvinyl chloride). Source-drain current modulation occurs via changes in the fluid gate potential by utilizing a pH-sensitive solid-state electrode (see Figure 1a and Supporting Information Figure S-2). Additionally, usage of FETs as biosensors allows scientists to leverage decades of research and billions of dollars in investment in computer chip processing/fabrication to expedite the development process. Sophisticated semiconductor fabrication foundries offered by companies such as Taiwan Semiconductor Manufacturing Company (TSMC) can manufacture devices with high yield, near-ideal and highly repeatable device characteristics with huge amenability for scale-up. For an excellent overview of ISFET operation, sensing modes, and important experimental design factors, the reader is referred to a review by P. Bergveld.[15]

Recent years have seen advancements in use of ISFETs in commercial applications for detection of biological reaction byproducts, such as hydrogen ions, for detection of nucleic acid amplification.[11,16] Although first introduced in the early 1990s,[17] DNA Electronics has come to the forefront of developing and commercializing this technique. In 2001, Toumazou et al. demonstrated detection of nucleotide incorporation events through detection of hydrogen ions in up to 5 simultaneous reactions.[10,11,18] This work has extended to sequencing applications and is currently utilized by Ion Torrent owned by Life Technologies. To date, commercial ISFET applications have required the use of a macroscale Ag/AgCl reference electrode to apply the necessary fluid gate biasing for FET operation. Although Rothberg et al. demonstrated a FET-based DNA sequencing system utilizing massively parallel nucleotide incorporation detection with millions of reaction wells using a single reference electrode,[19] this assay is limited to reactions that occur in pulses through sequential addition of nucleotides. Nucleic acid amplification techniques, such as PCR or loop mediated isothermal amplification (LAMP), require much longer time courses during which diffusion of hydrogen ions away from a noncompartmentalized reaction would limit parallel detection.

dx.doi.org/10.1021/ac500897t | Anal. Chem. 2014, 86, 6968−6975

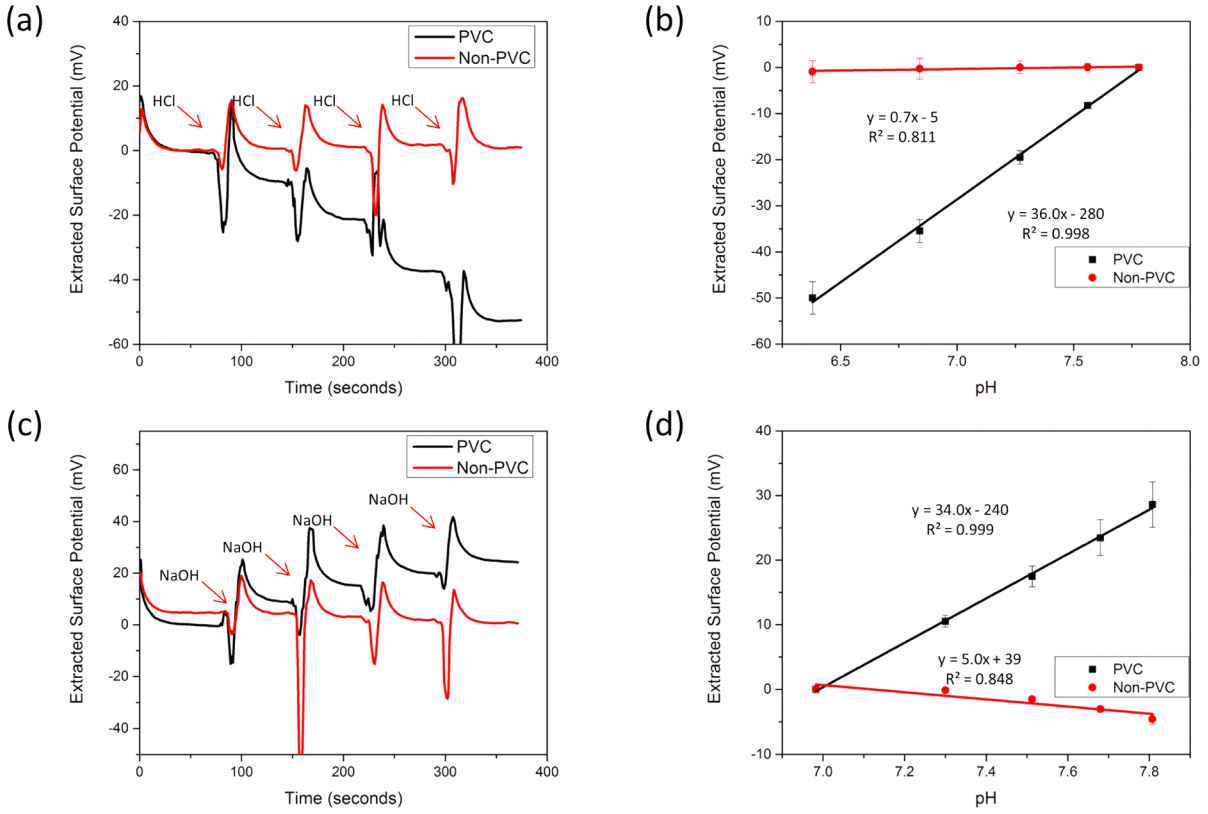

Figure 2. FET response with platinum fluid gate. (a) A real-time pH response curve of a PVC and non-PVC device with 4 subsequent HCl additions is shown. The non-PVC ISFET shows almost zero response when operated by the platinum electrode. (b) The pH response is quantified for many devices across multiple chips (n = 3). The PVC REFET sensor shows an apparent opposite trend than expected with hydrogen addition. This is due to the charge at the platinum electrode being mirrored into the REFET response. (c) A real-time pH response curve with four subsequent NaOH additions is shown. (d) The pH response is quantified across multiple devices (n = 3). The non-PVC ISFET shows minimal pH response compared to the PVC-REFET.

Use of an on-chip microfabricated electrode with encapsulation of each reaction volume can enable the parallel detection of many individual reactions, completely eliminating crosstalk between reaction chambers by physically isolating them from one another.

Here we detail the steps required to realize a methodology toward this goal. Because of the pH-sensitivity of solid-state electrodes,[20,21] a REFET design was used. An ISFET with a pH-passivating membrane monitored the pH response of the electrode. Previous techniques have demonstrated the use of pH-insensitive layers over ISFETs, such as silanes, buffered hydrogels, parylene, and polyACE.[22] However, polyvinyl chloride (PVC) offers an attractive alternative because of its previously demonstrated simple fabrication process, robust pH insensitivity, and known compatibility with PCR with added BSA.[23−26] Together, the combined system of a pH-sensitive electrode and a pH-insensitive REFET offers an opportunity for on-chip electrical detection of biological reactions, such as LAMP, targeting a variety of pathogens.

EXPERIMENTAL SECTION

Device Fabrication. Taiwan Semiconductor Manufacturing Company (Hsinchu, Taiwan) used a standard foundry process to manufacture 0.18 μm node extended-gate field effect transistors on silicon-on-insulator as seen in Figure 1b. Metal 1 was deposited to make contact to the source,drain, and to serve as the extended gate area connected to the polygate region. Next, an interlayer dielectric (ILD1) was deposited. Vias in ILD1 were etched to form 40 μm by 40 μm openings over the extended gate structure and exterior source/drain electrode pads for probing. A layer of hafnium oxide was then deposited over the entire chip to form the oxide sensing membrane on the extended gate structure. At UIUC, 200 Å titanium/800 Å platinum electrodes that were used as the fluid gate contact were patterned on top of the hafnium oxide dielectric layer using standard photolithography, evaporation, and lift-off steps. For the on-chip REFET, the chip was first silanized using HMDS for 1 h at 140 °C. The chip was then cleaned of any excess HMDS using consecutive rinses of acetone, methanol, DI water, and isopropanol. A mixture of 60% PVC, 40% dinonylphtalate (DNP), suspended in 3 mL of tetrahydrofuran (THF) was used for passivating the REFET.[24] One microliter of PVC/DNP suspended in THF was then spotted on half the devices and baked at 80 °C for 1 h (see Figure 1c). Before chips were measured, a final, 1 min oxygen plasma step was used to standardize the chip surface and prime the platinum.

Experimental Setup for FET Measurements. Current measurements and applied biases were controlled using a Keithley 4200 semiconductor characterization system. Contact to the chip electrode pads was established using micromanipulators from The Micromanipulator Company. For fluid gate measurements, a 400 μL, 10:1 PDMS well was placed on the chip. For reference measurements, fluid gate biases were applied with a Ag/AgCl reference electrode (RE) (Warner Instruments). For quasi-reference measurements, a micromanipulator was used to contact the on-chip platinum electrode

dx.doi.org/10.1021/ac500897t | Anal. Chem. 2014, 86, 6968−6975

(QRE). For pH titration experiments, 2 mM Tris buffer at pH 7.06 was used. Subsequent additions of 0.1 M NaOH or HCl were used to vary the pH. Baseline measurements were taken with the reference electrode to characterize the TSMC chips with and without PVC (see Figure 1d and f)). Separate calibration experiments using an In-Lab Ultra Micro pH Probe from Mettler Toledo were completed to quantify the pH response from a given NaOH or HCl addition event (see Supporting Information Figure S-1).

FET Testing and Surface Potential Measurements. Initial I_D-V_G curves measuring drain current, while sweeping the fluid gate were extracted with first the reference electrode and then with the quasi-reference platinum electrode. For pH titrations, current vs time measurements were taken with the FET set in the linear regime. To standardize measurements for different devices, the measured current was compared to the baseline I_D-V_G curve to extract the extended gate surface potential (see Figure 1d and f and Figure 2).

To quantify the pH sensitivity of the platinum QRE, the surface potential of the QRE versus the RE was measured using the Keithley 4200. The open circuit potential between the pH-insensitive RE and the QRE was measured with two separate Source Measuring Units (SMUs). Without a final oxygen plasma treatment step, the pH response was unstable as shown in Supporting Information Figure S-3.

LAMP Optimization and On-Chip Detection. Initial proof-of-concept LAMP experiments were completed with the EIKEN kit for *Escherichia coli* O157:H7. Further experiments that required modification of the LAMP solution were based on LAMP formulations from New England BioLabs' recommendations for LAMP. Primers used for *E. coli* O26 are found here.[27] 25 μL of reaction mix consisted of 0.05×−2× Isothermal Amplification Buffer from New England BioLabs, 800 mM Betaine from Sigma-Aldrich, 50 mM KCl, 1.9 μM FIP and BIP primers, 0.24 μM F3 and B3, 0.96 μM Loop-F and Loop-B primers, 1× EvaGreen from Biotium, 6 units of Warmstart Bst 2.0 polymerase from New England BioLabs, 1.3 mM dNTPs from New England BioLabs, 5 mM $MgSO_4$ from Sigma-Aldrich, and template of our targeted *E. coli* O26 template.

Optimization of the reaction centered around three major areas: (1) Tris-HCl buffer concentration, (2) starting pH value, and (3) reaction temperature. Electrical detection of LAMP was carried out by first running part of the solution in an Eppendorf RealPlex qPCR system. After completion, the portion of solution that was not amplified was measured on the FET with either the RE or the QRE, followed immediately by the amplified solution. Importantly, to minimize electrostatic discharge effects when exchanging solutions, the micromanipulator tips were lifted off the device pads in between measurements. Electrostatic discharge events have been shown to cause large shifts in the device threshold voltage and should be minimized through personal and system grounding whenever possible.[28]

RESULTS AND DISCUSSION

Characterization of TSMC Chip. Utilizing a semiconductor foundry for fabrication of ISFETs offers several distinct advantages. With the fabrication control afforded by the semiconductor foundry, charge trapped in the hafnium dielectric was controlled through anneals to minimally affect device stability. Threshold voltage uniformity across devices was excellent and the standard deviation of the threshold voltage of each individual device over 5 sweeps from cutoff to saturation was on the order of 0.1−1 mV. Assuming a Nernstian pH response, this noise level should enable a pH resolution on the order of 0.005−0.05 pH units. Hafnium oxide, a high-k dielectric, that increases the coupling capacitance to the device for a given thickness, has been shown to provide near Nernstian pH response.[29] This was evident in the baseline pH testing shown in Figure 1e. The pH titration in real-time method over a relatively small pH range (pH 7−8), showed some instability likely due to inaccuracy while pipetting. However, simultaneous measurement of two devices as shown in Figure 1d demonstrates sensor response uniformity and stability even when testing across the 5 mm sensing region of the chip.

Characterization of PVC-REFET and Platinum Response. Researchers have explored the use of REFETs for pH sensing applications starting shortly after the first ISFET was introduced in the 1970s.[15] REFET enables the user to normalize for unexpected changes in electrode potential or device response that can originate from factors other than pH changes, such as temperature instabilities. Typically, a pH insensitive REFET is paired with an ISFET in a differential setup. Extensive work has focused on a reliable method for properly rendering the REFET pH insensitive. Early examples focused on minimizing the number of available protonation/deprotonation groups at the device surface via the introduction of a silane layer that covalently reacted with hydroxyl groups on the dielectric surface. This method has seen limited practice due to difficulty in occupying a high enough percentage of available groups. Bergveld et al. showed a reduction of pH response of the ISFET to form a pH-insensitive REFET required a 99.99% reduction of hydroxyl groups.[30] As shown by Tarasov et al., this requires a silanization procedure that takes up to 7 days in a vacuum oven.[31]

Other early methods, such as ion-blocking layers of photoresist or other polymers like parylene or PVC, have also been demonstrated.[32−34] These methods primarily rely on a macroscale Ag/AgCl reference electrode for the fluid gate, which is bulky, expensive, and difficult to fabricate. Microfabricated Ag/AgCl electrodes also suffer from potential instability and reduced lifetime when submerged in solutions less than 3 M chloride.[35] Many examples have utilized a solid-state electrode as the fluid gate, but each used a differential signal between the ISFET and a REFET for pH sensing.[15,36] By elucidating the platinum pH response in Tris buffer, as seen in Figure 3, this work eliminated the need for a differential signal with an ISFET. By blocking the ISFET's pH response with spotted PVC, the resulting current trace from the ISFET shows the pH response of the platinum. When using the same surface potential extraction method as the baseline case, the sensor shows the opposite signal to the addition of NaOH or HCl (Figure 2). This overall pH sensitive system (~34−36 mV/pH) responds to the change in potential at the platinum fluid electrode and not the gate dielectric surface potential (see Supporting Information Figure S2). Each case demonstrated a linear relationship between the pH and the REFET response. Future steps will focus on metals with demonstrated higher pH sensitivity and more stable response, such as iridium or ruthenium.[37] When the QRE platinum electrode is used in conjunction with a device without PVC, the surface potential response of the platinum and the gate dielectric mirror each other. This results in a lack of pH sensitivity in the system for this case.

dx.doi.org/10.1021/ac500897t | *Anal. Chem.* 2014, 86, 6968−6975

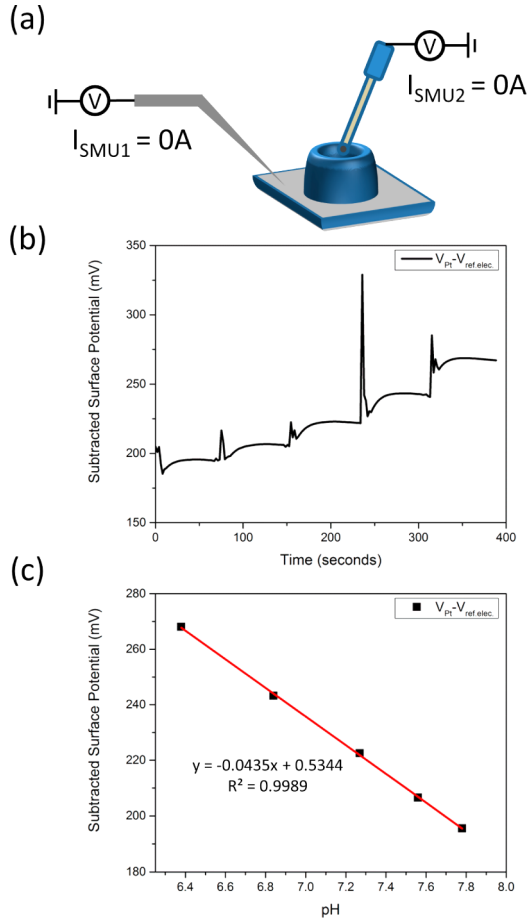

Figure 3. Platinum surface potential response. (a) A schematic of the open circuit potential method is shown. A PDMS well is placed on a platinum surface and Tris-HCl is added. The on-chip platinum (SMU1) vs the reference electrode (SMU2) is measured using the Keithley 4200 semiconductor characterization system. The current for both electrodes is held at zero and the resulting potential between the two nodes was measured. (b) A real-time plot of four HCl additions is shown. (c) The surface potential from the platinum response is extracted and quantified. The pH response shows high linearity and sensitivity that closely resembles those stated previously.[37]

Additionally, we have shown that the PVC membrane and solid-state electrode can be used for pH detection in droplets-in-mineral oil (see Supporting Information Figure S-4). It was noticed that PVC would delaminate from the chip surface upon submersion in mineral oil. This issue was accelerated at elevated temperatures; however, by baking the PVC at 80 °C before submersion, the PVC is able to maintain integrity for over 3 h at room temperature and over 1 h at 65 °C (Supporting Information Figure S-5). Prior work has also demonstrated PVC's compatibility in PCR applications;[26] however, this technique is most advantageous when used to determine the pH change associated with very high yield, lower temperature isothermal processes, such as LAMP. Nevertheless, the addition of additives[38] or in this case, baking the PVC to increase its thermostability in mineral oil adds the potential for droplet applications, such as digital PCR, that have gained popularity in recent years.[3]

LAMP versus PCR. Loop-mediated isothermal amplification (LAMP) was developed in the early 2000s as an isothermal alternative to PCR.[39,40] LAMP utilizes four distinct primers recognizing six regions of a targeted gene. This method offers high sensitivity (shown in Figure 4a) and superior specificity to PCR, which enables an inherently nonspecific method of amplification detection, such as an intercalating dye or, in this case, pH detection. Additionally, LAMP provides a yield of >500 μg/mL of DNA. PCR, on the other hand, only offers a maximum yield of around 40 μg/mL.[40] The level of DNA generation in LAMP results in a higher potential pH change for a given buffer concentration. Theoretically, in standard buffered amplification solution of 20 mM Tris-HCl, LAMP will yield a pH change of ∼−0.136 units, whereas PCR will only produce a pH change of ∼-0.01 units. (See Supporting Information for a description of the pH change calculations.) As shown in Figure 4b, using the Eiken kit for *E. coli* O157:H7, the LAMP reaction generates a pH change ranging from −0.15 to −0.20 pH units. This change is consistent across the entire range of starting template concentration since each reaction was allowed to run to completion.

Optimization of LAMP Reaction Conditions. The LAMP optimization process with respect to pH changes focused on three major areas: (1) Tris-HCl concentration, (2) starting pH value, and (3) reaction temperature. In a traditional amplification reaction, a highly buffered solution maintains a consistent pH in order to maximize polymerase activity. For a pH-based amplification reaction, the buffering capacity must be reduced, ideally without hindering polymerase activity. Figure 4c shows the pH change from LAMP versus a range of Tris-HCl concentrations, revealing the yield and pH change is consistent with expectations from 40 to 8 mM. The 4 mM reduced yield of the LAMP reaction slightly diminished the pH change. This behavior may be explained by the reduction in initial pH associated with diluting the buffer with DI water. When the starting pH was increased to around pH 8, the yield increased and followed expectations more closely.

Dilution of the isothermal amplification buffer also reduced the ionic strength of the solution. Without replacing the missing salts, the melting temperature of the dsDNA in solution decreases. As shown in Figure 4d, lower buffered solutions required a lower reaction temperature to see threshold times similar to higher buffered solutions. In the case of the 4 mM solution, the addition of 50 mM KCl increased the ionic strength of the solution and improved the threshold times observed. (data not shown).

End-Point Detection of LAMP On-Chip. Toumazou et al. previously demonstrated the potential for pH-based detection of nucleic acid amplification using an ISFET.[10,11,18] However, their system requires a reference electrode to establish the fluid gate potential and operate the ISFET. This technique is demonstrated in end-point measurement form in Supporting Information Figure S-6. This method advances the potential for portable nucleic acid amplification detection; however, on-chip reference electrodes are still fairly large and difficult to integrate with a microchip, making it nearly impossible to achieve massively parallel, portable amplification detection. By utilizing a solid-state electrode, patterned with standard photolithography and evaporated onto the chip, we added the potential for massively parallel amplification detection.

To demonstrate this potential, we have shown detection of a LAMP reaction using end-point pH measurements with a solid-state electrode and an ISFET passivated with PVC. Macroscale pH measurements with the In-Lab Ultra Micro pH meter showed a pH change of −1.24 units for the complete full reaction. As shown in Figure 5b and c, without the PVC membrane, the positive and negative amplification reactions are

dx.doi.org/10.1021/ac500897t | *Anal. Chem.* 2014, 86, 6968−6975

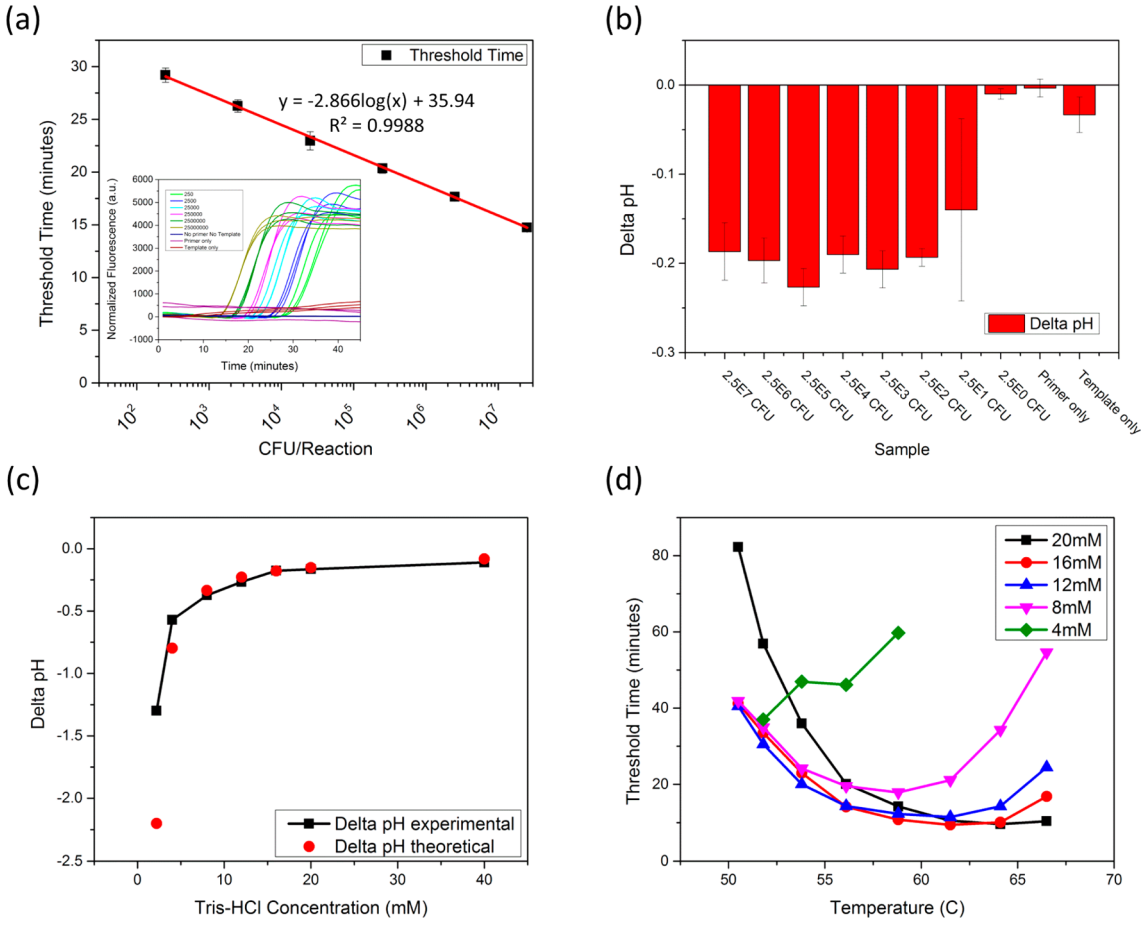

Figure 4. pH-LAMP optimization. (a) The detection limit of a commercially available *E. coli* O157:H7 kit is shown. LAMP allows for detection of 100−1000 CFU/reaction in less than 30 min. The inset graph provides the normalized real-time amplification data. (b) The pH-LAMP detection limit is shown. Regardless of starting *E. coli* concentration, the resulting pH change is consistent at around −0.2 pH units. (c) Reducing the Tris-HCl buffer concentration in the reaction mix increases the pH change associated with amplification. The maximum pH change observed in these tests was −1.2 pH units. (d) Decreasing the isothermal amplification buffer concentration also reduced the ionic strength of the solution. This requires the reaction temperature to be reduced to achieve consistent threshold times. Threshold times were consistent down to 8−12 mM Tris-HCl before significant increases in threshold time are observed.

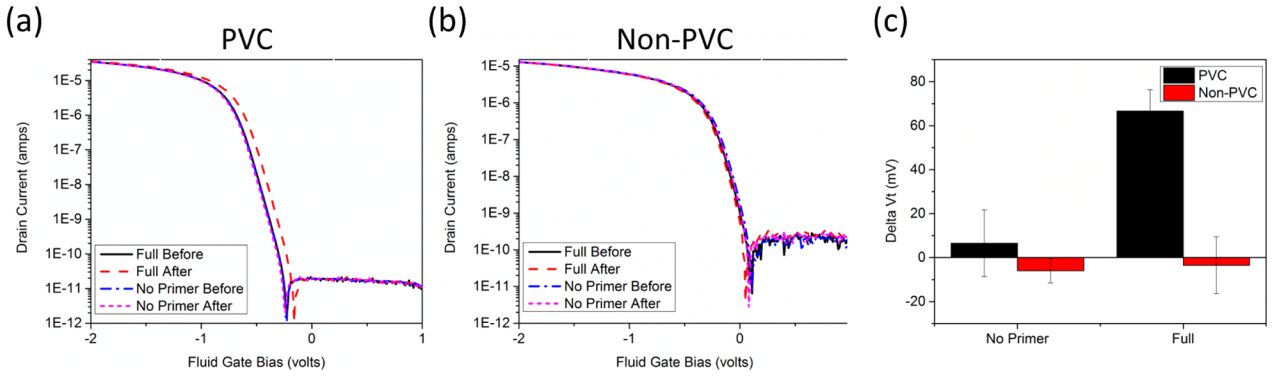

Figure 5. End point detection of LAMP on-chip. (a) *I*−*V* curves of a PVC-REFET device are shown. The differences between the negative control before and after amplification are not significant. The positive control shows a shift to a higher threshold voltage, which is consistent with a decrease in pH. The pH change was measured to be −1.2 units with a commercial meter. (b) Measurements were taken simultaneously with a non-PVC ISFET. The positive and negative amplification solutions show insignificant differences. (c) The change in threshold voltage was quantified for multiple devices. The change for positive amplification was statistically significant (n = 3, p-value < 0.01) when compared to the negative control for the PVC-REFET. The non-PVC ISFET showed no significant changes.

indistinguishable (two-tailed p-value = 0.7745). Compared to the negative reaction, the PVC REFET shows strong results that are statistically significant (p-value < 0.01). The PVC-REFET responds to the change in the electrode potential, which is sensitive to the pH of the solution. Supporting Information Figure S-7 shows the stability of the device

dx.doi.org/10.1021/ac500897t | *Anal. Chem.* 2014, 86, 6968−6975

threshold voltage with repeated solution exchanges. The LAMP end-point data was statistically significant compared to variations in the threshold voltage associated with solution exchange (p-value < 0.0001).

CONCLUSIONS

Here, we present a novel technique for electrical detection of nucleic acid amplification. Utilizing a field effect transistor in conjunction with a solid-state electrode simplifies ISFET pH-based detection of biological processes, such as macroscale LAMP. By incorporating simple to fabricate solid-state microelectrodes on the surface of a chip, droplets can be individually interrogated and their changing properties mapped. Disciplines that could see significant benefit from this methodology include digital PCR or digital LAMP, as well as assays enabled by electrowetting-on-dielectric droplet manipulations. Researchers could use this to perform high throughput analysis of enzyme activity, detect the presence of a targeted nucleic acid sequence, or detect the presence of a targeted biomolecule through monitoring an enzymatic reaction's rate and progress through hydrogen generation. This methodology enables droplet interrogation and simplifies macro-scale solution interrogation through the use of common metal patterning techniques and a pH-insensitive REFET.

ASSOCIATED CONTENT

Supporting Information

Additional material as described in the text. This material is available free of charge via the Internet at http://pubs.acs.org.

AUTHOR INFORMATION

Corresponding Author

*Address: 1270 Digital Computer Laboratory, Urbana, Illinois, USA, 61801. Tel: +01-217-333-1867. E-mail: rbashir@illinois.edu.

Author Contributions

E.S. and Y.Z. performed the experiments. E.S. and R.B. wrote the manuscript. E.S., B.R., and R.B. planned the experiments. V.S. and C.D. prepared devices at UIUC. Y.-S.L. planned and fabricated devices at TSMC.

Notes

The authors declare no competing financial interest.

ACKNOWLEDGMENTS

The authors would like to thank Lauren Yang for editing the manuscript. We would also like to thank Dr. Arun Bhunia, Dr. Titiksha Dikshit, and Dr. Atul Kumar Singh for helping prepare the biological samples and Koshin Hamasaki for helpful discussions. R.B. also acknowledges funding support from a cooperative agreement with Purdue University and the Agricultural Research Service of the United States Department of Agriculture, project number 1935-42000-035, and a subcontract to the University of Illinois at Urbana−Champaign. We also acknowledge support from NIH Grant R01-CA20003 and NSF I/IUCRC CABPN (Center for Agricultural, Biomedical and Pharmaceutical Nanotechnology) Grant at UIUC. We also acknowledge Taiwan Semiconductor Manufacturing Company for providing the ISFET chips and funding this work through project 2012-06536.

REFERENCES

(1) Saiki, R. K.; Gelfand, D. H.; Stoffel, S.; Scharf, S. J.; Higuchi, R.; Horn, G. T.; Mullis, K. B.; Erlich, H. A. *Science* **1988**, *239*, 487−491.
(2) Zhang, C.; Xu, J.; Ma, W.; Zheng, W. *Biotechnol. Adv.* **2006**, *24*, 243−284.
(3) Baker, M. *Nat. Methods* **2012**, *9*, 541−544.
(4) *Xxpress PCR*; BJS Biotechnologies: Greenford, Middlesex, U.K., 2014.
(5) RainDance Technologies, 2014. http://raindancetech.com/.
(6) Bio-Rad, 2014. http://www.bio-rad.com/.
(7) Gudnason, H.; Dufva, M.; Bang, D. D.; Wolff, A. *Nucleic Acids Res.* **2007**, *35* (19), No. e127, DOI: 10.1093/nar/gkm671.
(8) Xiang, Q.; Xu, B.; Li, D. *Biomed. Microdevices* **2007**, *9*, 443−449.
(9) Chin, C. D.; Linder, V.; Sia, S. K. *Lab. Chip* **2012**, *12*, 2118−2134.
(10) Kalofonou, M.; Toumazou, C. *Sens. Actuators, B* **2013**, *178*, 572−580.
(11) Toumazou, C.; Shepherd, L. M.; Reed, S. C.; Chen, G. I.; Patel, A.; Garner, D. M.; Wang, C. J. A.; Ou, C. P.; Amin-Desai, K.; Athanasiou, P.; Bai, H.; Brizido, I. M. Q.; Caldwell, B.; Coomber-Alford, D.; Georgiou, P.; Jordan, K. S.; Joyce, J. C.; La Mura, M.; Morley, D.; Sathyavruthan, S.; Temelso, S.; Thomas, R. E.; Zhang, L. *Nat. Methods* **2013**, *10*, 641−646.
(12) Veigas, B.; Branquinho, R.; Pinto, J. V.; Wojcik, P. J.; Martins, R.; Fortunato, E.; Baptista, P. V. *Biosens. Bioelectron.* **2014**, *52*, 50−55.
(13) Salm, E.; Liu, Y.-S.; Marchwiany, D.; Morisette, D.; He, Y.; K. Bhunia, A.; Bashir, R. *Biomed. Microdevices* **2011**, *13*, 973−982.
(14) Ghindilis, A. L.; Smith, M. W.; Schwarzkopf, K. R.; Zhan, C.; Evans, D. R.; Baptista, A. M.; Simon, H. M. *Electroanalysis* **2009**, *21*, 1459−1468.
(15) Bergveld, P. *Sens. Actuators, B* **2003**, *88*, 1−20.
(16) Credo, G. M.; Su, X.; Wu, K.; Elibol, O. H.; Liu, D. J.; Reddy, B.; Tsai, T. W.; Dorvel, B. R.; Daniels, J. S.; Bashir, R.; Varma, M. *Analyst* **2012**, *137*, 1351−1362.
(17) Sakurai, T.; Husimi, Y. *Anal. Chem.* **1992**, *64*, 1996−1997.
(18) Purushothaman, S.; Toumazou, C.; Georgiou, J. *IEEE Int. Symp. Circuits Syst.* **2002**, *4*, 169−172.
(19) Rothberg, J. M.; Hinz, W.; Rearick, T. M.; Schultz, J.; Mileski, W.; Davey, M.; Leamon, J. H.; Johnson, K.; Milgrew, M. J.; Edwards, M.; Hoon, J.; Simons, J. F.; Marran, D.; Myers, J. W.; Davidson, J. F.; Branting, A.; Nobile, J. R.; Puc, B. P.; Light, D.; Clark, T. A.; Huber, M.; Branciforte, J. T.; Stoner, I. B.; Cawley, S. E.; Lyons, M.; Fu, Y.; Homer, N.; Sedova, M.; Miao, X.; Reed, B.; Sabina, J.; Feierstein, E.; Schorn, M.; Alanjary, M.; Dimalanta, E.; Dressman, D.; Kasinskas, R.; Sokolsky, T.; Fidanza, J. A.; Namsaraev, E.; McKernan, K. J.; Williams, A.; Roth, G. T.; Bustillo, J. *Nature* **2011**, *475*, 348−352.
(20) Fog, A.; Buck, R. P. *Sens. Actuators* **1984**, *5*, 137−146.
(21) Kurzweil, P. *Sensors (Switzerland)* **2009**, *9*, 4955−4985.
(22) Bergveld, P.; Van Den Berg, A.; Van Der Wal, P. D.; Skowronska-Ptasinska, M.; Sudhölter, E. J. R.; Reinhoudt, D. N. *Sens. Actuators* **1989**, *18*, 309−327.
(23) Lee, Y. C.; Sohn, B. K. *J. Korean Phys. Soc.* **2002**, *40*, 601−604.
(24) Lai, C. S.; Lue, C. E.; Yang, C. M.; Dawgul, M.; Pijanowska, D. G. *Sensors* **2009**, *9*, 2076−2087.
(25) Errachid, A.; Bausells, J.; Jaffrezic-Renault, N. *Sens. Actuators, B* **1999**, *60*, 43−48.
(26) Kodzius, R.; Xiao, K.; Wu, J.; Yi, X.; Gong, X.; Foulds, I. G.; Wen, W. *Sens. Actuators, B* **2012**, *161*, 349−358.
(27) Wang, F.; Jiang, L.; Yang, Q.; Prinyawiwatkul, W.; Ge, B. *Appl. Environ. Microbiol.* **2012**, *78*, 2727−2736.
(28) Baldi, A.; Bratov, A.; Mas, R.; Domínguez, C. *Sens. Actuators, B* **2001**, *80*, 255−260.
(29) Dorvel, B. R.; Reddy, B.; Go, J.; Duarte Guevara, C.; Salm, E.; Alam, M. A.; Bashir, R. *ACS Nano* **2012**, *6*, 6150−6164.
(30) van den Berg, A.; Bergveld, P.; Reinhoudt, D. N.; Sudhölter, E. J. *Sens. Actuators* **1985**, *8*, 129−148.
(31) Tarasov, A.; Wipf, M.; Bedner, K.; Kurz, J.; Fu, W.; Guzenko, V. A.; Knopfmacher, O.; Stoop, R. L.; Calame, M.; Schönenberger, C. *Langmuir* **2012**, *28*, 9899−9905.

(32) Fujihira, M.; Fukui, M.; Osa, T. *J. Electroanal. Chem.* **1980**, *106*, 413−418.
(33) Skowronska-Ptasinska, M.; Van der Wal, P. D.; Van den Berg Bergveld, A. P.; Sudholter, E. J. R.; Reinhoudt, D. N. *Anal. Chim. Acta* **1990**, *230*, 67−73.
(34) Chang, K. M.; Chang, C. T.; Chao, K. Y.; Chen, J. L. *J. Electrochem. Soc.* **2010**, *157*, J143−J148.
(35) Waleed Shinwari, M.; Zhitomirsky, D.; Deen, I. A.; Selvaganapathy, P. R.; Jamal Deen, M.; Landheer, D. *Sensors* **2010**, *10*, 1679−1715.
(36) Wong, H.-S.; White, M. H. *IEEE Trans. Electron Devices* **1989**, *36*, 479−487.
(37) Kreider, K. G.; Tarlov, M. J.; Cline, J. P. *Sens. Actuators, B* **1995**, *28*, 167−172.
(38) Wypych, G. *PVC Degradation & Stabilization*; ChemTec Publishing: Toronto, Canada, 2008.
(39) Notomi, T.; Okayama, H.; Masubuchi, H.; Yonekawa, T.; Watanabe, K.; Amino, N.; Hase, T. *Nucleic Acids Res.* **2000**, *28* (12), No. e63, DOI: 10.1093/nar/28.12.e63.
(40) Nagamine, K.; Watanabe, K.; Ohtsuka, K.; Hase, T.; Notomi, T. *Clin. Chem.* **2001**, *47*, 1742−1743.